Conference materials
UDC 681.782.473
DOI: https://doi.org/10.18721/JPM.183.235

# InAsSb solid solution optocouple for carbon dioxide analysis

R.E. Kunkov✉, S.A. Karandashev, A.A. Klimov, T.S. Lukhmyrina, M.A. Remennyi

Ioffe Institute, St. Petersburg, Russia

✉ kunkov.re@mail.ioffe.ru

**Abstract.** This paper reports the results of work aimed at improving the performance of LEDs and photodiodes based on InAsSb solid solutions operating in the spectral range around 4.2 μm, as well as improving the efficiency of optocouple based on them in the absorption band of carbon dioxide in a wide temperature range, including high temperatures. An increase in the characteristics of optoelectronic components was achieved: detectivity $D^* = 3 \cdot 10^{10}$ (cm·$\sqrt{\text{Hz}}$)/W and LEDs' power ~ 100 μW (200 mA) at room temperature. Based on the obtained optoelectronic components, a non-dispersive infrared carbon dioxide sensor with a limit of detection of 0.0025 vol.%, relative error of 0.1% of measurement in the 0–10 vol.% concentration was developed. The sensor featured a 2 cm optical path, a sampling interval of 128 ms, and a power consumption of less than 50 mW.

**Keywords:** InAsSb heterostructures, mid-wave IR LEDs, mid-wave IR photodiodes, nondispersive infrared gas sensor

**Citation:** Kunkov R.E., Karandashev S.A., Klimov A.A., Lukhmyrina T.S., Remennyi M.A., InAsSb solid solution optocouple for carbon dioxide analysis, St. Petersburg State Polytechnical University Journal. Physics and Mathematics. 18 (3.2) (2025) 178–182. DOI: https://doi.org/10.18721/JPM.183.235



Материалы конференции
УДК 681.782.473
DOI: https://doi.org/10.18721/JPM.183.235

# Оптопары на основе твердых растворов InAsSb для детектирования углекислого газа

Р.Э. Кунков✉, С.А. Карандашев, А.А. Климов, Т.С. Лухмырина, М.А. Ременный

Физико-технический институт им. А.Ф. Иоффе РАН, Санкт-Петербург, Россия

✉ kunkov.re@mail.ioffe.ru

**Аннотация.** Сообщается о результатах работы, нацеленной на улучшение характеристик свето- и фотодиодов на основе полупроводников InAsSb, работающих в средневолновой ИК области спектра около 4.2 мкм, а также на повышении эффективности их работы как оптопары в полосе поглощения углекислого газа в широком интервале температур.

На основе представленных оптопар был разработан недисперсионный инфракрасный датчик углекислого газа.

**Ключевые слова:** гетероструктуры InAsSb, средневолновые ИК светодиоды, средневолновые ИК фотодиоды, недисперсионный инфракрасный газовый датчик

**Ссылка при цитировании:** Кунков Р.Э., Карандашев С.А., Климов А.А., Лухмырина Т.С., Ременный М.А., Оптопары на основе твердых растворов InAsSbp для детектирования углекислого газа // Научно-технические ведомости СПбГПУ. Физико-математические науки. 2025. Т. 18. № 3.2. С. 178–182. DOI: https://doi.org/10.18721/JPM.183.235



## Introduction

The first symptoms of the negative effect of $CO_2$ on the human body begin already at concentrations of about 0.1–0.15 % vol. Therefore, the permissible levels of carbon dioxide in industrial, office and residential buildings are strictly regulated. Non-dispersive infrared gas sensors based on LEDs and photodiodes are effective devices for gas analysis, characterized by high selectivity, long lifetime and sensitivity down to ppm units [1]. The requirements for such sensors are constantly increasing, resulting in the need to find solutions for: minimizing power consumption, size and weight of the sensor (SWaP minimization); increasing the efficiency of the optoelectronic components used; integration of optoelectronic and related electronic components.

To date, the most widely used sensors are those based on thermal sources and infrared (IR) radiation detectors [2], which typically exhibit high power consumption, low response speed, and relatively low sensitivity. Medium-wave IR photodiodes and optically excited light-emitting diodes (LEDs) based on lead salts [3] have also been employed in sensor development. However, their key drawback is the lack of long-term parameter stability.

A promising alternative to these devices is IR sensors utilizing light-emitting diodes (LEDs) and photodiodes (PDs) based on $A^3B^5$ semiconductors, particularly InAsSb(P) solid-solution heterostructures, which offer high metallurgical stability and relatively low cost. For many years, IR optoelectronics laboratory of the Ioffe Institute has been developing and studying optoelectronic components based on diode heterostructures with an active layer of $InAs_{1-x}Sb_x$ solid solution, including those operating in the ~ 4.2 μm wavelength range [4–6], as well as optical sensors derived from them [7]. The objectives of this study were: improving the performance of optoelectronic components (LEDs and PDs); enhancing their efficiency as optopairs over a wide temperature range; developing a compact, non-dispersive $CO_2$ sensor with a high level of integration of optical, optoelectronic, and electronic components.

## Results and Discussion

The studied LED and photodiode samples were fabricated from an *n*-InAsSbP/$InAsSb_x$/*p*-InAsSbP heterostructure with an active/photosensitive $InAsSb_x$ ($x = 0.08$) region 4–3 μm thick, grown by LPE on $n^+$-InAs (100) substrates. The key design features of the LEDs and photodiodes included: a flip-chip configuration with an active/photosensitive area diameter of ~140 μm and light input/output through a 20–40 μm substrate; immersion coupling of the chip with a 3.5 mm Si lens featuring an antireflection coating.

For the experimental LED and photodiode samples (LED42 and PD42), (Fig. 1, *a*, *b*) presents the electroluminescence spectra at a 200 mA pumping current in CW mode and the photosensitivity across a significantly extended temperature range of 200–500 K compared to prea viously published results. The photodiode's current responsivity and the LED's output power were also increased [7], achieved through optimization of the epitaxial structure design. Specifically, reducing the thickness of the active/photosensitive region minimized self-absorption of radiation and lowered the dark current.

In addition to the main optopair, the sensor incorporated a reference-channel photodiode (PD38) and two interference filters (IF42 and IF38), which split and filtered the LED42 emission to create the measurement (LED42-IF42-PD42) and reference (LED42-IF38-PD38) channels. Fig. 1, *c* shows the normalized spectral characteristics of these components at room temperature, along with the $CO_2$ transmission spectrum in the operational wavelength range.

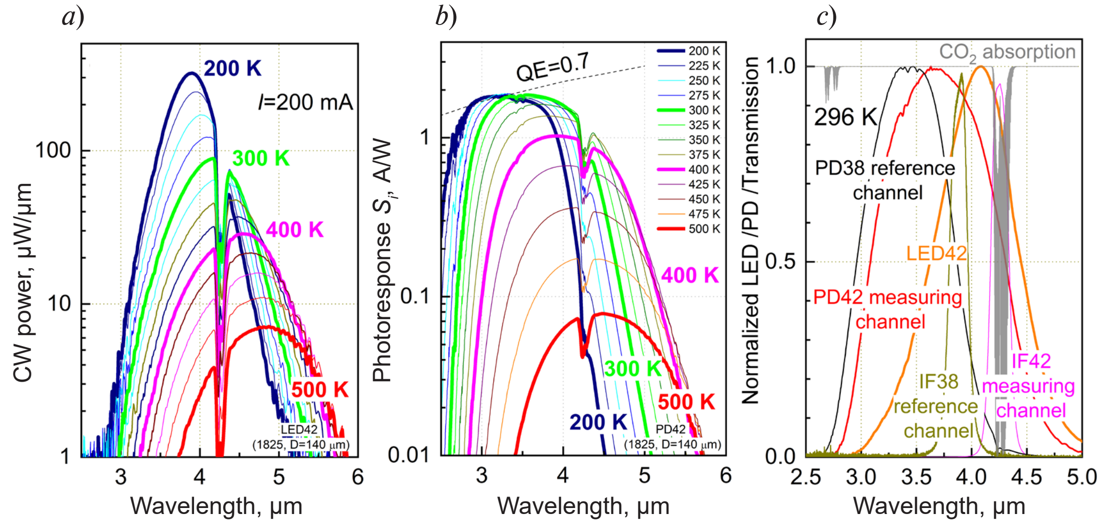


Fig. 1. Electroluminescence spectra (*a*) and current responsivity (*b*) in the temperature range of 200–500 K; normalized spectral characteristics of the optoelectronic components used and $CO_2$ transmission (*c*)

Based on the obtained temperature dependencies of zero bias resistance (Fig. 2, *a*), the noise characteristics of photodetectors PD42 and PD38 were calculated, as well as the total noise at the output of (photodiode) + (first-stage op-amp) system. The calculation was performed for a frequency bandwidth $\Delta f = 1$ Hz, $f > 10$ kHz (i.e., outside the $1/f$ noise region) using Eq. (1) [8]:

$$I_{n\_\Sigma}(\Delta f) = \Delta f \cdot \sqrt{i^2_{n\_PD} + i^2_{OP} + i^2_{fb}} = \Delta f \cdot \sqrt{\frac{4kT}{R_o} + i^2_{n\_OP} + \left(\frac{e_{n\_OP}}{R_o}\right)^2 + \frac{4kT}{R_{fb}}}\,[A], \quad (1)$$

where the first term represents photodiode noise; the second and third terms correspond to the first-stage operational amplifier (op-amp) noise; and the last term represents the thermal noise of the feedback resistance in the first amplification stage. As seen in Fig. 2, *a*, the op-amp contributes significantly to the total noise, particularly at the extremes of the temperature range: at elevated temperatures, the dominant contribution comes from the op-amp's voltage noise ($e_{n\_OP}$), while at lower temperatures, the current noise ($i_{n\_OP}$) prevails.

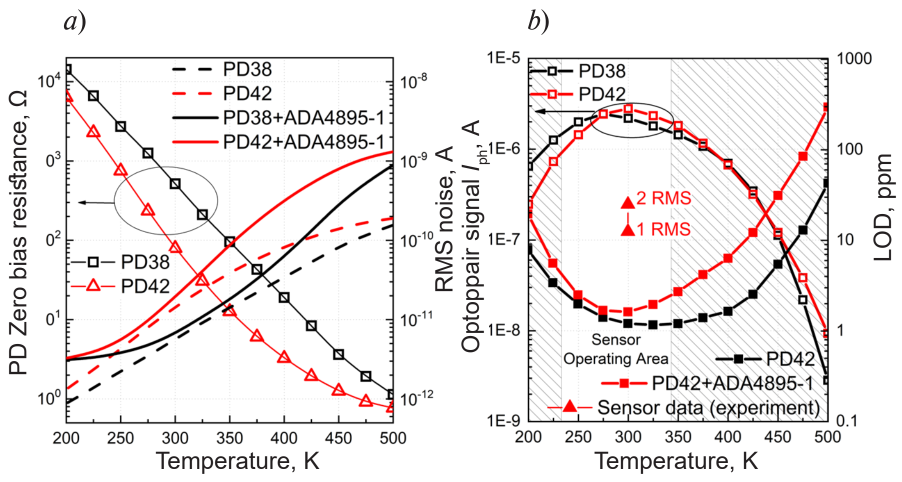


Fig. 2. Temperature dependences for zero bias resistance and RMS noises of photodiodes both individually and in the op-amp circuit (*a*), and integrated optopair signals at 200 mA LED drive current and limit of detection, ppm (*b*)

Fig. 2, *b* shows the temperature dependencies of the optopair signals for the measurement and reference channels, calculated using Eq. 2:

$$I_{ph} = \int_{\lambda_1}^{\lambda_2} P_{LED}(\lambda) \cdot T_{IFx}(\lambda) \cdot S_{IPDx}(\lambda) d\lambda, \quad (2)$$

where $P_{LED}(\lambda)$ is the spectral power distribution of LED42, $T_{IFx}(\lambda)$ is the transmission spectrum of the interference filter, and $S_{IPDx}(\lambda)$ is the current responsivity spectrum of the photodiode for the respective optopair.

To evaluate the limit of detection (LOD), the sensor's transfer function was calculated by introducing an additional multiplicative factor in Eq. 2 accounting for infrared absorption by $CO_2$ at a 2 cm optical path length:

$$I_{ph} = \int_{\lambda_1}^{\lambda_2} (1 - \exp(-k(\lambda) \cdot C \cdot d)) \cdot P_{LED42}(\lambda) \cdot T_{IF42}(\lambda) \cdot S_{IPD42}(\lambda) d\lambda, \quad (3)$$

where $k(\lambda)$ is the spectral absorption coefficient of $CO_2$ (data from the HITRAN database), $C$ is the gas concentration in vol.%, and $d$ is the optical path length.

Fig. 2, *b* shows the calculated LOD for carbon dioxide in the temperature range of 200–500 K, derived from the obtained signal and noise dependencies along with the sensor's transfer function (assuming its minimal temperature variation). The calculation was performed for a frequency bandwidth of $\Delta f = 1$ Hz. Experimental values obtained at room temperature during prototype testing (see Fig. 3) are also presented.

*a*) *b*) *c*)

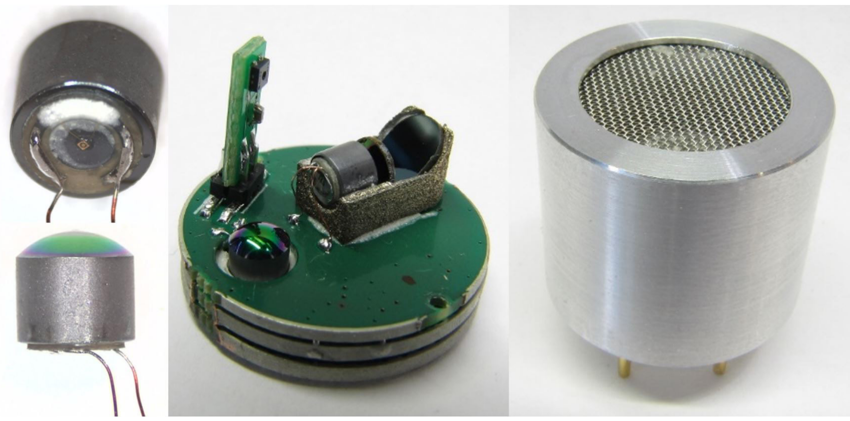

Fig. 3. Photographs of immersion light-emitting diodes and photodiodes (left), sensor during intermediate assembly (center), and fully packaged device in a ⌀20×16 mm housing (right)

The root-mean-square (RMS) noise was estimated at 15 ADC counts, with the useful signal ranging from 37127 to 85940 ADC counts. The LOD (defined as 2×RMS, corresponding to 95% confidence level for normally distributed errors) reached ≈ 0.0025 vol.% (25 ppm). The relative measurement error did not exceed 0.1 % of the measured value across concentrations up to 10 vol.%.

A comparison of the prototype sensor's characteristics with commercially available counterparts [2, 3] demonstrated its superior performance in response speed (6–30 times faster), LOD (up to 2 times lower), and dynamic range (over 2 times wider).

**Conclusion**

The paper presents the results of work on the development of LEDs and photodiodes based on InAsSb/InAsSbP heterostructures and NDIR carbon dioxide sensor operating in the mid-wave IR region of the spectrum. For the design of immersion LEDs and photodiodes with a wavelength of about 4.2 μm, the values of detectability $D^* = 3 \cdot 10^{10}$ (cm·√Hz)/W and LED power ~100 μW (CW current 200 mA) at room temperature are obtained. The NDIR carbon dioxide sensor with an optical path length of about 2 cm and average power consumption of 25 mW was characterized by a carbon dioxide limit of detection of 0.0025 vol.% and a relative measurement error of 0.1% in the concentration range up to 10 vol.%.

## REFERENCES


1. **Kochelaev E.A., Petrov V.V.**, Design of a compact optical carbon monoxide sensor with a threshold sensitivity of 1 mg/m3 (0.85 ppm). Evaluation of measurement selectivity, Optics and Spectroscopy.131 (10) (2023) 1359.
2. “Dynament” (UK) NDIR gas sensors. [Electronic resource]. URL: http://www.dynament.ru/pdf/tds0048.pdf
3. “Optosense” (RU) NDIR gas sensors [Electronic resource]. URL: https://optosense.ru/upload/iblock/212/ESAT.100700.00%20%D0%A0%D0%AD.pdf
4. **Zotova N.V., Ilyinskaya N.D., Karandashev S.A., et al.,** 4.2 μm flip-chip LEDs with deep etch mesa, Semiconductors. 4 (6) (2006).
5. **Zakheim A.L., Zotova N.V., Ilyinskaya N.D., et al.,** Uncooled wideband flip-chip photodiodes based on InAsSb ($\lambda_{cut\ off}$ = 4.5 μm), Semiconductors. 43 (3) (2009).
6. **Ilyinskaya N.D., Karandashev S.A., Karpuhina N.G., et al.,** Photodiode 1 × 64 linear array based on a double *p*-InAsSbP/*n*-$InAs_{0.92}Sb_{0.08}$/$n^+$-InAs heterostructure, Semiconductors. 50 (5) (2016) 657.
7. **Sotnikova G.Yu., Gavrilov G.A., Aleksandrov S.E., et al.,** Low Voltage $CO_2$-Gas Sensor Based on III–V Mid-IR Immersion Lens Diode Optopairs: Where we Are and How Far we Can Go, IEEE Sensors Journal. 10 (2) (2010) 225–234.
8. **Gavrilov G.A., Matveev B.A., Sotnikova G.Yu.,** Maximum sensitivity of a photodetector based on A3B5 photodiodes of the mid-IR spectrum range, Semiconductors. 37 (18) (2011) 50 – 57.


## THE AUTHORS


**KUNKOV Roman E.**
Kunkov.re@mail.ioffe.ru
romunkov@yandex.ru
ORCID: 0000-0002-2377-2287

**KLIMOV Aleksandr A.**
a.klimov@ioffe.mail.ru
ORCID: 0000-0001-5642-0483

**KARANDASHEV Sergey A.**
ksa08@yandex.ru
ORCID: 0000-0002-0255-7123

**LUKHMYRINA Tatyana S.**
h7k9g00@gmail.com
ORCID: 0000-0002-3989-6487

**REMENNYI Maxim A.**
Mremennyy@mail.ioffe.ru
ORCID: 0000-0002-4735-9681


*Received 15.09.2025. Approved after reviewing 25.09.2025. Accepted 30.09.2025.*